Finally, the EXAFS results give us a clue for understanding the magnetic properties of the intercalates, particularly the occurrence of spontaneous magnetization at low temperature; this magnetization has been ascribed to weak ferromagnetism,[6,17] a phenomenon that takes place when antiferromagnetically coupled spins do not align themselves exactly antiparallel, the canting resulting in an uncompensated macroscopic moment. The results described in the present study strongly suggest either that neighbor manganese ions see different environments or that the environments do not have the same orientation: as a consequence, the preferred directions of neighbor spins will not be parallel. Basically, the reason is that the "single-ion-anisotropy energy" is different for the same orientation of a spin at the two sites and that the total energy is minimized by a nonparallel arrangement.[18] This explanation seems more realistic than an invocation of antisymmetric exchange between the spins, which may be another source of canting. Although it is always very difficult to sort out the relative contributions of the two possible mechanisms, antisymmetric exchange is known to be small for $Mn^{2+}$ ions, which have no first-order orbital magnetic contribution.

In conclusion, it turns out that EXAFS is a valuable technique to characterize local disorder in intercalated layers. Further EXAFS experiments on similar systems are in course, which should indicate whether the observed effects constitute a particular case or express some general feature of intercalation.

**Acknowledgment.** We thank the staff of the linear accelerator laboratory of Orsay, who operated the storage ring DCI for the synchrotron radiation dedicated shift used in this work. We also thank the staff of LURE, particularly those involved in the EXAFS spectrometer design. We are grateful to Dr. J. Goulon for his help in writing the EXAFS analysis programs and to Dr. R. Fourme for helpful discussions.

**Registry No.** I, 74346-92-2; II, 74346-93-3; $MnPS_3$, 20642-09-5.

(17) Clement, R.; Renard, J. P., to be submitted for publication.
(18) Carlin, R. L.; Van Duyneveldt, A. J. "Magnetic Properties of Transition Metal Compounds"; Springer-Verlag: New York, 1977.
(19) Lee, P.; Beni, G. *Phys. Rev. B: Solid State* **1977**, *15*, 2862.

Contribution from the Department of Chemistry, McMaster University, Hamilton, Ontario, Canada L8S 4M1

# Vibrational Spectra and Analyses of the $S_4^{2+}$, $Se_4^{2+}$, $Te_4^{2+}$, and *trans*-$Te_2Se_2^{2+}$ Polyatomic Cations

ROBERT C. BURNS and RONALD J. GILLESPIE*

*Received February 2, 1982*

Raman and infrared spectra have been recorded on a number of compounds that contain the $S_4^{2+}$, $Se_4^{2+}$, $Te_4^{2+}$, and *trans*-$Te_2Se_2^{2+}$ polyatomic cations. In the case of $S_4^{2+}$ isotopic enrichment of sulfur to 16.1% in $^{34}S$ has been used to help assign the fundamental vibrations of this cation on the basis of a square-planar structure with $D_{4h}$ symmetry. Assignments have also been extended to the $Se_4^{2+}$ and $Te_4^{2+}$ cations. Differences with previous assignments are discussed. In the case of *trans*-$Te_2Se_2^{2+}$, assignments were made on the basis of a square-planar structure with $D_{2h}$ symmetry. Extensive vibrational analyses, using a modified valence force field, have been carried out on all of these species, giving chalcogen–chalcogen stretching force constants (average values) of 2.69, 2.09, 1.41, and 1.78 mdyn/Å for $S_4^{2+}$, $Se_4^{2+}$, $Te_4^{2+}$, and *trans*-$Te_2Se_2^{2+}$, respectively. These values have been compared to values for chalcogen–chalcogen single bonds and are consistent with an expected formal bond order of 1.25 for these species. A brief treatment of the data for $D_{4h}$ systems using central rather than valence force coordinates is also given.

## Introduction

The polyatomic cations $S_4^{2+}$, $Se_4^{2+}$, and $Te_4^{2+}$ and the polyatomic anion $Bi_4^{2-}$, each with 22 valence electrons, represent the only known examples of isolated homoatomic four-atom square-planar species that have $D_{4h}$ symmetry.[1,2] This type of structure is important from the standpoint of vibrational analysis because of its inherent simplicity and has been treated on a theoretical basis by a number of researchers.[3,4] However, the only extensive treatments using normal-coordinate methods based on experimental work have been those by Gillespie and Pez,[5] and by Steudel[6] (who used the former's results) on the $Se_4^{2+}$ cation. The rather limited extent to which the vibrational spectra of these species have been studied may, in part at least, be attributed to the difficulty in preparing compounds containing these species, which have been synthesized only in recent years. On the basis of the vibrational spectra obtained by Gillespie and co-workers, assignments have also been given for $S_4^{2+}$ and $Te_4^{2+}$, but no normal-coordinate analyses have been made for these species.[1,7]

In both of the previous studies of $Se_4^{2+}$ the vibrational data were interpreted in terms of the Urey–Bradley potential field and conflicting assignments were made for one of the fundamental modes of vibration. Furthermore, as part of a recent MO study of $Te_4^{2+}$ using an ab initio pseudopotential approach, theoretically derived (symmetrized) force constants and vibrational frequencies were obtained that suggested an alternative assignment of the observed frequencies for this cation.[8] The purpose of the present work was to reinvestigate the vibrational spectra of the $S_4^{2+}$, $Se_4^{2+}$, and $Te_4^{2+}$ cations and to carry out extensive vibrational analyses on each of these species. As an assist in the assignments isotopic substitution

(1) Gillespie, R. J.; Passmore, J. *Adv. Inorg. Chem. Radiochem.* **1975**, *17*, 49.
(2) Cisar, A.; Corbett, J. D. *Inorg. Chem.* **1977**, *16*, 2482.
(3) Pistorius, C. W. F. T. *Z. Phys. Chem. (Wiesbaden)* **1958**, *16*, 126.
(4) Cyvin, S. J. "Molecular Vibrations and Mean Square Amplitudes"; Elsevier: Amsterdam, 1968.
(5) Gillespie, R. J.; Pez, G. P. *Inorg. Chem.* **1969**, *8*, 1229.
(6) Steudel, R. *Z. Naturforsch., A* **1975**, *30A*, 1481.
(7) Gillespie, R. J.; Passmore, J.; Ummat, P. K.; Vaidya, O. C. *Inorg. Chem.* **1971**, *10*, 1327.
(8) Rothman, M. J.; Bartell, L. S.; Ewig, C. S.; Van Wazer, J. R. *J. Comput. Chem.* **1980**, *1*, 64.

0020-1669/82/1321-3877$01.25/0 

of sulfur enriched to 16.1% in $^{34}S$ was made in the case of $S_4^{2+}$, the only cation for which isotopic substitution would produce significant shifts in the frequencies of the vibrational modes.

Some mixed polyatomic cations containing sulfur, selenium, and tellurium are also known, and the related $Te_3Se^{2+}$, *cis*- and *trans*-$Te_2Se_2^{2+}$, and $TeSe_3^{2+}$ species have recently been characterized by $^{125}Te$ and $^{77}Se$ Fourier-transform NMR studies.[9,10] Furthermore, the structure of *trans*-$Te_2Se_2^{2+}$-$(Sb_3F_{14}^-)(SbF_6^-)$ has been determined and the *trans*-$Te_2Se_2^{2+}$ cation shown to have a square-planar structure, with effective $D_{2h}$ symmetry for an isolated cation.[11] In view of the close structural relationship of this heteropolyatomic cation to those of the homopolyatomic species described above, a vibrational study and analysis were also undertaken on this cation.

## Experimental Section

**Materials.** Sulfur (BDH, sublimed), selenium ("Baker Analyzed", J. T. Baker Chemical Co.), and tellurium (K & K, ICN Pharmaceuticals, 99.7%) were used directly as supplied. Arsenic pentafluoride (Ozark Mahoning Co.) was used directly from the cylinder. Antimony pentafluoride (Ozark Mahoning Co.) was doubly distilled in a Pyrex glass still under an atmosphere of dry nitrogen. Selenium tetrachloride (Alfa Inorganics, 99.5%) was used without further purification, while $TeCl_4$ (Alfa Inorganics, 99%) was sublimed under vacuum before use. Commercial $AlCl_3$ was purified by sublimation under vacuum after a prior sublimation from aluminum shot to remove the $FeCl_3$ impurity. Anhydrous $SO_2$ (Matheson of Canada) was distilled from a glass vessel containing $P_4O_{10}$, over which it had been stored for at least 24 h. Approximately 65% oleum was prepared by distilling $SO_3$ ("SULFAN", Allied Chemical Corp.) onto a weighed amount of commercial sulfuric acid (BDH, 95.5%), while 15–18% oleum ("Baker Analyzed", J. T. Baker Chemical Co.) was used as supplied.

Sulfur enriched to 16.1% in $^{34}S$ was obtained in the form of $Ag_2S$. This was dissolved in 8 M HCl over a period of 3 to 4 h, with heating, to give $H_2S$. With use of a flow of nitrogen, the $H_2S$ was continually swept into an oxidizing solution prepared from $NaVO_3$ (1.5× excess) and $Na_3$(citrate) (1.5× excess; this forms a 1:1 complex with V(IV), which is formed in the reaction) in 250 $cm^3$ of a $Na_2CO_3$ solution (10 g $dm^{-3}$) with the pH of the solution being adjusted to 9 by addition of solid $CO_2$.[12] This gave a satisfactory precipitate of rhombic rather than plastic sulfur. The precipitated sulfur was then filtered and extracted in a Soxhlet apparatus with freshly distilled cyclohexane ("Analar") and crystallized after removal of the majority of the solvent.

Peroxydisulfuryl difluoride ($S_2O_6F_2$) was kindly prepared by Dr. G. J. Schrobilgen, using the procedure of Wechsberg et al.,[13] and its purity was checked by density measurements and Raman spectroscopy.[14]

**Preparation of Salts of the $S_4^{2+}$, $Se_4^{2+}$, $Te_4^{2+}$, and *trans*-$Te_2Se_2^{2+}$ Cations.** The majority of compounds studied in this investigation were prepared according to their published procedures.[1,11,15-18] However, some slight differences were observed in the preparation of $S_4(SO_3F)_2$. This compound has been reported to form by reaction of sulfur and excess $S_2O_6F_2$ in $SO_2$ at low temperatures and has been described as a pale yellow or white solid.[7,15] In an identical preparation we observed that sulfur and $S_2O_6F_2$ (ca. 3× excess over that required to give $S_4^{2+}$) reacted to give a pale yellow insoluble compound as described previously but which, when the mixture was stirred for 10–14 days at room temperature, was replaced by a white solid that was marginally soluble in $SO_2$. Analytical and spectroscopic examination of both the pale yellow and white solids indicated that the former was the previously reported $S_4(SO_3F)_2$ but that the latter was the previously uncharacterized salt $S_4(S_2O_6F)_2$. Anal. Calcd for $S_4(SO_3F)_2$: S:F, 3.00. Found: S:F, 2.99. Calcd for $S_4(S_2O_6F)_2$: S, 52.73; F, 7.81; O, 39.46. Found: S, 52.78; F, 7.70; O (by difference), 39.52. Previously, both of these compounds had been described as $S_4(SO_3F)_2$ and it should be noted that the reported Raman spectrum[7] of this compound is actually that of $S_4(S_2O_6F)_2$.

The compound $KS_2O_6F$ was prepared according to the method of Lehmann and Kolditz,[19] and its identity was checked by X-ray powder methods.

**Spectra.** Raman spectra were obtained with a Spex 14018 0.85-m Czerny–Turner double-monochromator equipped with holographic gratings of 1800 grooves/mm. Slit width settings depended on properties such as the scattering efficiency of the sample and the laser power and ranged from about 75 to 350 μm in this study. An RCA C31034 phototube detector was used in conjunction with a pulse amplifier, analyzer and rate meter, all of which have been described previously,[20] and spectra were recorded on a Texas Instruments FS02WBA strip-chart recorder. The exciting radiation was either the red 6328-Å line of a Spectra-Physics Model 125 He–Ne laser or the green 5145-Å line of a Spectra-Physics Model 140 $Ar^+$ laser. Both solid and solution samples were contained in $^1/_4$ in. o.d. Pyrex tubes, and if thermally unstable, they were spun in a rotating cell to minimize decomposition.

Infrared spectra were recorded on a Perkin-Elmer Type 283 grating infrared spectrometer (4000–200 $cm^{-1}$) or on a Nicolet 7199 FT IR system (ca. 500–50 $cm^{-1}$) using 12.5 and 6.25 μm Mylar beam splitters. For the FT IR spectra, 600 or 900 scans were accumulated and the resulting spectra subjected to a five-point smoothing routine.[21] Both the Raman and FT IR data are accurate to ±1 $cm^{-1}$ over the range in which the bands were observed. Infrared samples were mounted as Nujol oil mulls, but as many of the compounds were found to attack this mulling agent, Fluorolube oil (Grade S30, Hooker Chemical Co.) was also employed. Other samples were mounted as finely ground powders between CsI or AgCl windows, or in thin polyethylene packets, which were heat sealed after the compounds had been introduced. Both the Nujol and Fluorolube oils had been dried and were stored over sodium.

Electronic diffuse-reflectance spectra (340–710 nm) were recorded against $MgCO_3$ on a Cary 14 instrument, equipped with a standard reflectance attachment. Samples were handled in a drybox and loaded into $^1/_4$ in. o.d. Pyrex tubes or airtight cells, similar to that described by Reid, Scaife, and Wailes.[22] X-ray powder diffraction data were obtained as described previously.[23]

**Analyses.** Analyses were carried out by Alfred Bernhardt Analytische Laboratorien, Elbach, West Germany.

## Results and Discussion

**Preparation of $S_4(SO_3F)_2$ and $S_4(S_2O_6F)_2$.** Reaction of sulfur with excess $S_2O_6F_2$ in $SO_2$ at low temperatures initially produced a pale yellow insoluble solid, which was shown by analysis and spectroscopic procedures to be $S_4(SO_3F)_2$. However, when the mixture was stirred for 10–14 days in the presence of excess $S_2O_6F_2$ in $SO_2$, the yellow solid was replaced by a white material that was found to be the previously unknown salt $S_4(S_2O_6F)_2$. Both compounds previously had been formulated as $S_4(SO_3F)_2$. The compound $S_4(SO_3F)_2$ contains the $SO_3F^-$ anion, while $S_4(S_2O_6F)_2$ contains the $S_2O_6F^-$ anion. The latter anion is derived from fluorodisulfuric acid, $HS_2O_6F$, which has been observed in the $HSO_3F$–$SO_3$ system where it was studied by Raman and $^{19}F$ NMR techniques.[24] Very few salts of fluorodisulfuric acid are known, but compounds described as complexes between ionic fluorides and $SO_3$, e.g., $KF{\cdot}2SO_3$ (i.e., $K^+S_2O_6F^-$), are in fact salts of this acid. The formation of $S_4(S_2O_6F)_2$ from $S_4(SO_3F)_2$ on prolonged reaction

(9) Schrobilgen, G. J.; Burns, R. C.; Granger, P. *J. Chem. Soc., Chem. Commun.* **1978**, 957.
(10) Lassigne, C. R.; Wells, E. J. *J. Chem. Soc., Chem. Commun.* **1978**, 956.
(11) Boldrini, P.; Brown, I. D.; Collins, M. J.; Gillespie, R. J.; Maharajh, E.; Slim, D. R.; Sawyer, J. F. *Inorg. Chem.*, in press.
(12) Hileman, O. E., personal communication, 1979.
(13) Wechsberg, M.; Bulliner, P. A.; Sladky, F. O.; Mews, R.; Bartlett, N. *Inorg. Chem.* **1972**, *11*, 3063.
(14) Qureshi, A. M.; Levchuk, L. E.; Aubke, F. *Can. J. Chem.* **1971**, *49*, 2544.
(15) Barr, J.; Gillespie, R. J.; Ummat, P. K. *J. Chem. Soc., Chem. Commun.* **1970**, 264.
(16) Barr, J.; Crump, D. B.; Gillespie, R. J.; Kapoor, R.; Ummat, P. K. *Can. J. Chem.* **1968**, *46*, 3607.
(17) Prince, D. J.; Corbett, J. D.; Garbisch, B. *Inorg. Chem.* **1970**, *9*, 2731.
(18) Cardinal, G.; Gillespie, R. J.; Sawyer, J. F.; Vekris, J. E. *J. Chem. Soc., Dalton Trans.* **1982**, 765.
(19) Lehmann, H. A.; Kolditz, L. *Z. Anorg. Allg. Chem.* **1953**, *272*, 69.
(20) Gillespie, R. J.; Schrobilgen, G. J. *Inorg. Chem.* **1976**, *15*, 22.
(21) Savitzky, A.; Golay, M. J. E. *Anal. Chem.* **1964**, *36*, 1627.
(22) Reid, A. F.; Scaife, D. E.; Wailes, P. C. *Spectrochim. Acta, Part A* **1964**, *20A*, 1257.
(23) Burns, R. C.; Gillespie, R. J.; Luk, W.-C. *Inorg. Chem.* **1978**, *17*, 3596.
(24) Gillespie, R. J.; Robinson, E. A. *Can. J. Chem.* **1962**, *40*, 675.

Table I. Electronic Absorption and Diffuse-Reflectance Spectra of the $Se_4^{2+}$ Cation in Different Environments[a,b]

| species | color | Se–Se dist, Å | $\pi \rightarrow \pi^*$ ($^1A_{1g} \rightarrow {}^1E_g$), nm | $\pi \rightarrow \pi^*$ ($^1A_{1g} \rightarrow {}^1E_g$) or $\pi \rightarrow n^*$ ($^1A_{1g} \rightarrow {}^1A_{1g}$, $^1B_{1g}$, $^1A_{2g}$, $^1B_{2g}$), nm[c] |
|---|---|---|---|---|
| $Se_4^{2+}$(soln)[d] | yellow | | 410 | 320 |
| $Se_4(Sb_2F_4)(Sb_2F_5)(SbF_6)_5$ | golden yellow | 2.257 (4), 2.264 (4)[f,g] | 413 | 382 sh[e] |
| $Se_4(AsF_6)_2$ | yellow | | 440 | 385 |
| $Se_4(AlCl_4)_2$ | yellow-orange | 2.283 (2), 2.288 (2)[f,g] | 488 | 430 |
| $Se_4(HS_2O_7)_2$ | orange | 2.283 (4)[h] | 524 | 428 |

[a] All spectra recorded at room temperature. [b] Diffuse-reflectance spectra recorded from 340 to 710 nm. [c] For a discussion of this assignment see ref 8 and 26. [d] Spectra recorded in highly acidic media such as $H_2S_2O_7$, $HSO_3F$, and oleum. [e] sh = shoulder. [f] Reference 18. [g] Two crystallographically independent cations. [h] Reference 27.

as described above is tentatively attributed to oxidation of the $SO_2$ solvent by the excess $S_2O_6F_2$ to give $SO_3$, which subsequently reacts with $SO_3F^-$ to give $S_2O_6F^-$. Presumably this reaction is fairly slow as $S_4(SO_3F)_2$ can be isolated as an intermediate product, while in previous studies using excess $S_2O_6F_2$ as oxidant in $SO_2$, only $SO_3F^-$ salts have been obtained.

The slight difference in color of the two $S_4^{2+}$ salts may be easily explained by a slight shift in the broad dipole-allowed $\pi \rightarrow \pi^*$ ($^1A_{1g} \rightarrow {}^1E_u$) transition of $S_4^{2+}$ at ca. 330 nm to lower energies in the case of $S_4(SO_3F)_2$, such that the tail of this band appears in the visible region. This would give rise to the slight yellow coloration. Similar differences in color have been observed for salts of $Se_4^{2+}$, viz., both $Se_4(Sb_2F_4^{2+})(Sb_2F_5^+)(SbF_6^-)_5$ and $Se_4(AsF_6)$ are yellow and $Se_4(AlCl_4)_2$ is yellow-orange, while $Se_4(HS_2O_7)_2$ is bright orange in color. This trend is associated with an increase in the Se–Se bond length (and hence a decrease in the energy of the $\pi \rightarrow \pi^*$ transition) in those salts with the more polarizable anion or, alternatively, the one providing the highest charge density (or ionic potential) around the cation.[25] For $Se_4^{2+}$, considerable spectroscopic and crystallographic data have been amassed that demonstrate this trend and are listed in Table I. We note immediately that there is a general decrease in the energy of the $\pi \rightarrow \pi^*$ transition with increasing Se–Se bond distance. Furthermore, all of these salts, as well as compounds of $S_4^{2+}$ and $Te_4^{2+}$, have fairly strong cation–anion interactions,[18] which, in conjunction with the above trend, is indicative of a trend in the extent of charge transfer (and hence covalent nature) between the anions and high-energy (antibonding) cation orbitals of appropriate symmetry. However, although the Se–Se bond distances in each of the two independent cations in $Se_4(AlCl_4)_2$ are not crystallographically distinguishable from that in $Se_4(HS_2O_7)_2$,[18] the respective $\pi \rightarrow \pi^*$ transitions in the two salts differ by 36 nm (Table I). Perhaps this may be related in one instance to the effect of differences in the potential field created by the respective anions. Further evidence for other differences between these compounds appear in the vibrational data, as shown below.

In the case of the $S_4^{2+}$ species, physical and spectroscopic studies (see below) suggest that $S_4(SO_3F)_2$ is somewhat more covalent than $S_4(S_2O_6F)_2$. Hence, we expect that the $\pi \rightarrow \pi^*$ transition should be found at relatively lower energies for the more covalent $S_4(SO_3F)_2$, which is consistent with the observed yellow color of the compound.

**Vibrational Spectra of the $S_4^{2+}$, $Se_4^{2+}$, $Te_4^{2+}$, and *trans*-$Te_2Se_2^{2+}$ Cations and Band Assignments.** For an isolated square-planar four-atom system with $D_{4h}$ symmetry the vibrational representation is $\Gamma_{vib} = A_{1g} + B_{1g} + B_{2g} + B_{2u} + E_u$, where the coordinate system is such that the $z$ axis is perpendicular to the plane containing the four atoms, and the $x$ and $y$ axes pass through diagonally opposed atoms. Such a $D_{4h}$ system has a center of inversion, and the mutual exclusion rule applies, so that the $A_{1g}$, $B_{1g}$, and $B_{2g}$ modes are only Raman active and the $E_u$ mode is only infrared active. These are all in-plane motions, for which there are $2N - 3 = 5$ normal modes of vibration ($N$ = number of atoms). The $B_{2u}$ mode, which describes the out-of-plane motion ($N - 3 = 1$), is neither Raman nor infrared active. As the normal modes of vibration are distributed one to each symmetry species, this particular geometry is one of the "diatomic-like" models referred to by Cyvin,[4] in which the secular determinant factors into linear equations, each of which may be formally treated as a diatomic molecule.

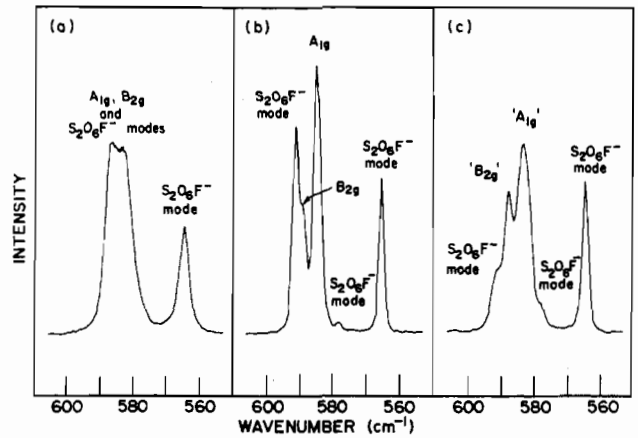


**Figure 1.** Raman spectra of $S_4(S_2O_6F)_2$ from 605 to 555 cm$^{-1}$ (a) at room temperature and (b) at −196 °C (both with natural-abundance sulfur) and (c) at −196 °C with sulfur in the cation enriched to 16.1% in $^{34}S$.

**The $S_4^{2+}$ Cation.** Raman and infrared spectra were recorded on both $S_4(S_2O_6F)_2$ and $S_4(SO_3F)_2$, while Raman spectra were also obtained on $S_4(S_2O_6F)_2$ in which the $S_4^{2+}$ cation had been enriched in $^{34}S$. Assignments have been made for both compounds, but some difficulty was experienced in providing a definite assignment for a number of the vibrational modes of the cations and anions in $S_4(SO_3F)_2$, due to their close proximity and hence overlap.

For $S_4(S_2O_6F)_2$ the Raman data (at −196 °C), infrared data (at room temperature), and band assignments are listed in Table II, together with data on $KS_2O_6F$ and $HS_2O_6F$. The Raman spectra (605–555 cm$^{-1}$) of $S_4(S_2O_6F)_2$ at room temperature and at −196 °C with natural-abundance sulfur (ca. 95.8% $^{32}S$) in the cation and the Raman spectrum at −196 °C with sulfur in the cation enriched to 16.1% in $^{34}S$ are shown in Figure 1. For the natural-abundance material, comparison of the Raman spectra at room temperature and at −196 °C

(25) Burns, R. C.; Gillespie, R. J.; Barnes, J. A.; McGlinchey, M. J. *Inorg. Chem.* **1982**, *21*, 799.
(26) Tanaka, K.; Yamabe, T.; Terama-e, H.; Fukui, K. *Inorg. Chem.* **1979**, *18*, 3591.
(27) Brown, I. D.; Crump, D. B.; Gillespie, R. J. *Inorg. Chem.* **1971**, *10*, 2319.

Table II. Vibrational Data ($cm^{-1}$) and Assignments for $S_4(S_2O_6F)_2$, $KS_2O_6F$, and $HS_2O_6F$[a,b]

| $S_4(S_2O_6F)_2$ | | $KS_2O_6F$[d] | $HS_2O_6F$ | |
|---|---|---|---|---|
| Raman (−196 °C) | IR[c] | IR[c] | Raman ($HSO_3F$ soln)[e] | assignt |
| 1434 (4) | ~1430 s, br[f] | 1440 m | 1489 | |
| 1304 (5) | ~1310 s, sh | 1385 m | 1412 | |
| 1243 (23) | ~1250 s, br | 1310 s | 1241 | ν(SO) |
| 1233 (17) | ~1230 s, sh | 1265 s | 1212 | |
| 1220 (1) | 1221 s, br | 1200 m | | |
| | | | 1160 | OH wag |
| 1071 (14) | 1062 m | 1078 m | 1080[g] | ν(SO) |
| | | 1043 m | | |
| | | | 973 | ν(S–OH) |
| 863 (4) br | 875 m | 855 m | 850 | ν(SF) |
| | 830 m | 783 m | | |
| 712 (6) | 700 w, br | 737 m | 721 | $\nu_{as}$(S–O–S) |
| 634 (2) | 628 w | 648 w | | $\nu_s$(S–O–S) |
| 592 (~20)[h] | 593 w | 617 w? | 562 | $SO_2$ bend |
| 590 (~50)[h] | | | | $\nu_3(B_{2g})$ $S_4^{2+}$ |
| 585 (100) | | | | $\nu_1(A_{1g})$ $S_4^{2+}$ |
| 578 (4) | | | | ? |
| 566 (56) | 568 m, sh | 564 s | 550 | $SO_2$ bend |
| | 542 m | | | $\nu_5(E_u)$ $S_4^{2+}$ |
| 530 (7) | 526 m | 506 m | | $SO_2$ rock |
| 459 (3) | 456 w | 451 w | 458 | S–F wag |
| 434 (1) | 435 w | | | ? |
| 383 (6) | | | | $\nu_2(B_{1g})$ $S_4^{2+}$ |
| 338 (8) | 335 m, sp | 330 w | 325 | $SO_2$ rock |
| 315 (8) | 311 m | 300 w | 311 | S–F wag |
| 299 (7) | 297 m | 278 m | 300 | torsion |
| | 257 w, sp | | | ? |
| 181 (1) | | | | ? |
| 140 (15) | | | | lattice mode |
| 138 (17) | | | 140 | SOS bend |
| 136 (4) sh | | | | |
| 116 (6) | | | | |
| 104 (26) | | | | |
| 98 (5) | | | | |
| 87 (9) | | | | lattice modes |
| 77 (4) | | | | |
| 73 (12) | | | | |
| 65 (1) | | | | |
| 56 (6) | | | | |
| 38 (5) br | | | | |

[a] Spectra recorded at room temperature unless otherwise indicated. [b] Raman intensities in parentheses. [c] Infrared spectrum not recorded below 200 $cm^{-1}$. [d] All attempts to obtain a good Raman spectrum of $KS_2O_6F$ at room temperature or at −196 °C were unsuccessful. [e] Reference 24. [f] Key: s = strong, m = medium, w = weak, br = broad, sp = sharp, sh = shoulder. [g] Band from $S_2O_6F^-$ added to $HS_2O_6F$.[24] [h] Intensities are based on the resolved components in the envelope.

shows that considerably better resolution is obtained at the lower temperature. Indeed, it was only by recording the spectrum at low temperatures and by isotopic substitution, as shown below, that the $B_{2g}$ mode was identified.

For spectra recorded at −196 °C, isotopic substitution indicates that only three bands change in height, width, and position relative to the anion bands[28]—there is no scrambling of the $^{34}S$ between the cation and anion. Thus, in the spectrum of the material obtained with natural-abundance sulfur in the cation, these bands must correspond to the three Raman-active modes $A_{1g}$, $B_{1g}$, and $B_{2g}$. The band at 585 $cm^{-1}$ is by far the most intense and is accordingly assigned as the $A_{1g}$ mode. Although no polarization measurements could be performed in solution as the compound is only slightly soluble in $SO_2$, assignment of this mode as $A_{1g}$ is in agreement with polarization measurements on the $Se_4^{2+}$ and $Te_4^{2+}$ cations. The weak band at 383 $cm^{-1}$ is assigned $B_{1g}$ symmetry (it involves only angle-bending motions), while that at 590 $cm^{-1}$ is assigned $B_{2g}$ symmetry. This latter mode overlaps slightly with an anion vibration at 592 $cm^{-1}$ in the spectrum of the natural-abundance sample, but in the spectrum of the sample enriched in $^{34}S$, the $A_{1g}$ and $B_{2g}$ cation bands are shifted by ca. 1.5 $cm^{-1}$ to lower frequencies as well as being considerably broader[28] and are now resolvable (see Figure 1b,c). This is the first time that the $B_{2g}$ vibrational mode has been definitely identified for any of the square-planar $M_4^{2+}$ (M = S, Se, Te) cationic species.

In the infrared spectrum of $S_4(S_2O_6F)_2$ none of the three Raman-active cation modes appears although a band is observable at 593 $cm^{-1}$. However, this band is attributed to the same anion mode that is observed in the Raman spectrum (at 592 $cm^{-1}$). Because of the low symmetry of the anion ($C_1$) every vibration is Raman and infrared active. Therefore the infrared band at 542 $cm^{-1}$, which has no Raman-active counterpart, is assigned as the $E_u$ mode of the cation. This is also in agreement with assignments for the $Se_4^{2+}$ and $Te_4^{2+}$ cations.

In this study no detailed assignments of the $S_2O_6F^-$ anion were made, but rather, assignments were taken from those reported by Gillespie and Robinson[24] for $HS_2O_6F$ and the $S_2O_6F^-$ anion in $HSO_3F$ solution and the assignments of the related $S_2O_7^{2-}$ anion (with an assumed $C_2$ symmetry) by Brown and Ross.[29] These assignments must therefore be regarded as tentative. More definite assignments would require an extensive study of other simple salts containing this anion, in conjunction with normal-coordinate calculations.

For $S_4(SO_3F)_2$ the Raman and infrared data (at room temperature) and band assignments are given in Table III. Assignments were made on the basis of isolated ions, but the available evidence, both physical and spectroscopic, indicates that this compound is fairly covalent in nature. As indicated above, $S_4(SO_3F)_2$ is essentially insoluble in $SO_2$, a medium in which salts of polyatomic cations are generally soluble. Also, $S_4(SO_3F)_2$ sublimes above ca. 250 °C, unlike $S_4(S_2O_6F)_2$,

Table III. Raman and Infrared Data ($cm^{-1}$) and Assignments for $S_4(SO_3F)_2$[a]

| Raman[b] | IR[c] | assignt |
|---|---|---|
| 1294 (5) br | ~1290 s, sh[d] | $\nu_4$(E) $SO_3F^-$ |
| 1226 (17) | 1230 vs | |
| 1072 (44) | 1070 s, sp | $\nu_1(A_1)$ $SO_3F^-$ |
| 744 (2) br | 755 s, br | $\nu_2(A_1)$ $SO_3F^-$ |
| 733 (1) | 736 s, br | |
| 603 (47) | | $\nu_3(B_{2g})$ $S_4^{2+}$ |
| 589 (100) | | $\nu_1(A_{1g})$ $S_4^{2+}$ |
| 576 (71) | 579 s, sp | $\nu_3(A_1)$ and $\nu_5$(E) $SO_3F^-$, and $\nu_5(E_u)$ $S_4^{2+}$ |
| 564 (94) | 567 s | |
| 556 (6) sh | 560 m, sh | |
| | 549 m | |
| | 530 m | |
| 408 (2) | 407 m, sp | $\nu_6$(E) $SO_3F^-$ |
| 398 (3) | 397 m, sp | |
| 382 (9) | | $\nu_2(B_{1g})$ $S_4^{2+}$ |
| 142 (40) | | lattice and cation–anion interaction modes (?) |
| 130 (24) | | |
| 116 (17) | | |
| 109 (9) | | |
| 76 (8) | | |
| 58 (11) br | | |
| 37 (10) | | |

[a] Data reported for spectra recorded at room temperature. For $S_4^{2+}$, Raman data at −196 °C are $A_{1g}$ = 591 (100), $B_{1g}$ = 383 (7), and $B_{2g}$ = 604 (51) $cm^{-1}$. [b] Raman intensities given in parentheses. [c] Infrared spectrum not recorded below 200 $cm^{-1}$. [d] Key: vs = very strong, s = strong, m = medium, w = weak, br = broad, sp = sharp.

(28) The observed increases in bandwidth and the shifts to lower frequencies are due to overlap of the modes of $^{32}S_4^{2+}$ with the appropriate modes of the isotopic isomers of $(^{34}S_x{}^{32}S_{4-x})^{2+}$, primarily $(^{34}S^{32}S_3)^{2+}$ in this case.

(29) Brown, R. G.; Ross, S. D. *Spectrochim. Acta, Part A* **1972**, *28A*, 1263.

Table IV. Raman and Infrared Data ($cm^{-1}$) and Assignments for $Se_4^{2+}$ in Solution and in Various Compounds[a]

| $Se_4^{2+}$ (65% oleum) Raman[b] | $Se_4(Sb_2F_4)(Sb_2F_5)$-$(SbF_6)_5$ Raman | | $Se_4(AsF_6)_2$ | | | $Se_4(HS_2O_7)_2$ | | | $Se_4(AlCl_4)_2$ | | | |
|---|---|---|---|---|---|---|---|---|---|---|---|---|
| | | | Raman | | IR | Raman | | IR | Raman | | IR | |
| | −196 °C | RT | −196 °C | RT | RT | −196 °C | RT | RT | −196 °C | RT | RT | assignts |
| *f* | *f* | *f* | *f* | *f* | | 329 (71) | 326 (23) | | 301 (70) | 298 (37) | | $\nu_3(B_{2g})$ |
| 326 (100) pol[c] | 327 (100) | 326 (100) | 326 (100) | 324 (100) | | 324 (100) | 322 (100) | | 317 (100) | 312 (100) | | $\nu_1(A_{1g})$ |
| | | | 307 (1) | ... | 308 | 306 (3) | 303 (1) | 302 | ~306 (2) sh | 303 (2) sh | 301 | $\nu_5(E_u)$ |
| | *d* | 302 (3)? | | | | | | | | | | |
| | | | 302 (1) | 302 (1) br | 303 | 294 (3) | 293 (1) | 294 | 292 (2) | 288 (3) | 289 | |
| 187 (5) dp | 182 (2) | 180 (2) | 181 (2) | 180 (2) | | 189 (8) | 188 (9) | | 183 (3)[e] | 180 (2)[e] | | $\nu_2(B_{1g})$ |

[a] Raman intensities given in parentheses. [b] Solution data recorded at room temperature. [c] Key: pol = polarized, dp = depolarized, br = broad, sh = shoulder. [d] Obscured by a broad $\nu$(Sb–F) stretch at ~285 $cm^{-1}$. [e] Overlapped to some extent by $\nu_3(T_2)$ of $AlCl_4^-$. [f] $\nu_3(B_{2g})$ is estimated to be <~1 $cm^{-1}$ different from $\nu_1(A_{1g})$; see text.

Table V. Raman and Infrared Data ($cm^{-1}$) and Assignments for $Te_4^{2+}$ in Solution and in Various Compounds[a,b]

| $Te_4^{2+}$ (15% oleum) Raman | $Te_4(AsF_6)_2$ | | $Te_4(SbF_6)_2$ | | $Te_4(AlCl_4)_2$ | | $Te_4(Al_2Cl_7)_2$ | | |
|---|---|---|---|---|---|---|---|---|---|
| | Raman | IR | Raman | IR | Raman | IR | Raman | IR | assignts[e] |
| 217 (100) pol[c] | 213 (100)[d] | | 214 (100)[d] | | 212 (100)[d] | | 211 (100)[d] | | $\nu_1(A_{1g})$, $\nu_3(B_{2g})$[e] |
| | | 186 w | | 187 | | *f* | | *f* | $\nu_5(E_u)$ |
| 107 (8) dp | 103 (10) | | 106 (12) | | 104 (19) | | 102 (18) | | $\nu_2(B_{1g})$ |

[a] All data reported on spectra recorded at room temperature. Raman data at −196 °C are little different from those reported at room temperature. [b] Raman intensities given in parentheses. [c] Key: pol = polarized, dp = depolarized, w = weak. [d] Resonance Raman bands ($2\nu_1$, $3\nu_1$) are observed at frequency values of ~424 (20) and ~638 (7) $cm^{-1}$ for all compounds. [e] $\nu_3(B_{2g})$ is estimated to be <~1 $cm^{-1}$ different from $\nu_1(A_{1g})$; see text. [f] $\nu_5(E_u)$ is obscured by $\nu_3(T_2)$ of the $AlCl_4^-$ anion and a similar band in $Al_2Cl_7^-$.

which decomposes on heating. These properties are indicative of a rather covalent nature. The spectroscopic data for $S_4(SO_3F)_2$ also support this conclusion. Although the splitting of the anion modes could simply be attributed to a reduction in site symmetry of the anion, the appearance, splitting, and frequency shift of the anion bands are similar to those observed in cases where coordination of $SO_3F^-$ has been postulated.[30] The splitting of $\nu_2$, which has $A_1$ symmetry, also suggests that there may be more than one crystallographic site (of different symmetry) for the $SO_3F^-$ anion. Similar splittings of the doubly degenerate $\nu_4$, $\nu_5$, and $\nu_6$ modes and doubling of these and other modes of $A_1$ symmetry have also been observed in the spectra of covalent mono- and bis(fluorosulfate) complexes of many transition metals, very often accompanied by the appearance of fairly strong cation–anion interaction modes.[30,31]

The $B_{2g}$ mode for the $S_4^{2+}$ cation in $S_4(SO_3F)_2$ is 14 $cm^{-1}$ to higher frequencies than the $A_{1g}$ mode, whereas in $S_4(S_2O_6F)_2$ this difference is only 5 $cm^{-1}$. A slightly greater difference, 17 $cm^{-1}$, has been observed between these modes in $S_4(AsF_6)_2 \cdot 0.6SO_2$.[32] It is therefore apparent that the $B_{2g}$ mode can shift quite markedly with respect to the $A_{1g}$ mode, depending on the particular compound. Further discussion of this behavior is given below.

**The $Se_4^{2+}$ and $Te_4^{2+}$ Cations.** For the $Se_4^{2+}$ and $Te_4^{2+}$ cations Raman spectra were recorded on solutions containing these species, together with polarization measurements, while both Raman and infrared spectra were recorded on the solid compounds $Se_4(AsF_6)_2$, $Se_4(Sb_2F_4)(Sb_2F_5)(SbF_6)_5$, $Se_4(AlCl_4)_2$, $Se_4(HS_2O_7)_2$, $Te_4(AsF_6)_2$, $Te_4(SbF_6)_2$, $Te_4(AlCl_4)_2$, and $Te_4(Al_2Cl_7)_2$. A summary of the data for both cations is given in Tables IV and V. Complete data for these compounds are not given as we are primarily interested in the cation vibrations, and those of many of the anions have been reported elsewhere.[5,17,23,33] Except where noted in Tables IV and V, there was no overlap between cation and anion bands. Raman spectra (at −196 °C) for $Se_4(AsF_6)_2$, $Se_4(HS_2O_7)_2$, and $Se_4(AlCl_4)_2$ from 360 to 270 $cm^{-1}$ are reproduced in Figure 2.

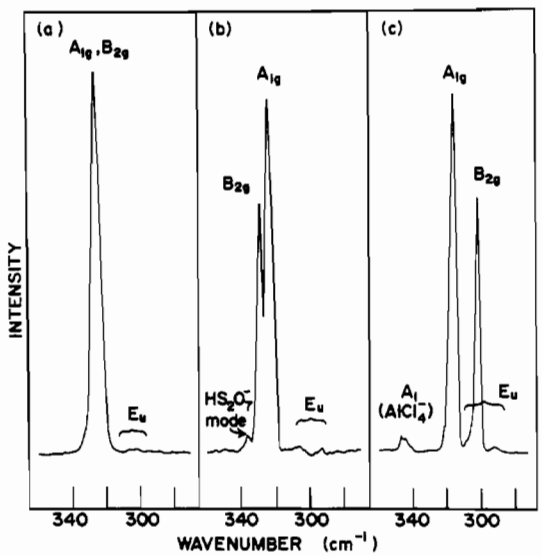


**Figure 2.** Raman spectra at −196 °C of (a) $Se_4(AsF_6)_2$, (b) $Se_4(HS_2O_7)_2$, and (c) $Se_4(AlCl_4)_2$ from 360 to 270 $cm^{-1}$.

Except for $Se_4(HS_2O_7)_2$ and $Se_4(AlCl_4)_2$ the $B_{2g}$ mode was not observed in any of the Raman spectra of the $Se_4^{2+}$ or $Te_4^{2+}$ compounds at room temperature or at −196 °C although in, for example, $Se_4(AsF_6)_2$, evidence for considerable asymmetry to the high-frequency side of the $A_{1g}$ peak was noted. All attempts to resolve the latter peak into two separate peaks were unsuccessful, even with a resolution of 1 $cm^{-1}$. Since the separation of the $B_{2g}$ and $A_{1g}$ modes, although small, is likely to be at least 1 $cm^{-1}$ in some cases, it is at first sight somewhat surprising that they cannot be resolved. However, the large numbers of isotopes of moderately high abundance for both selenium and tellurium cause all bands to be fairly broad (from overlap of isotopic isomers) so that resolution is in fact impossible for either cation.

In the case of $Se_4(AlCl_4)_2$ the fairly intense band at 298 $cm^{-1}$ could alternately be assigned as the $B_{2g}$ mode or as part of a

(30) Goubeau, J.; Milne, J. B. *Can. J. Chem.* **1967**, *45*, 2321.
(31) Alleyne, C. S.; Mailer, K. O.; Thompson, R. C. *Can. J. Chem.* **1974**, *52*, 336.
(32) Passmore, J.; Sutherland, G., personal communication, 1980.
(33) Nakamoto, K. "Infrared and Raman Spectra of Inorganic and Coordination Compounds", 3rd ed.; Wiley-Interscience: New York, 1978.

Table VI. Summary of Vibrational Data ($cm^{-1}$) for the $S_4^{2+}$, $Se_4^{2+}$, and $Te_4^{2+}$ Polyatomic Cations[a]

| | $S_4^{2+}$ | | $Se_4^{2+}$ [b] | | | $Te_4^{2+}$ | | |
|---|---|---|---|---|---|---|---|---|
| species | this work | ref 7 | this work | ref 5 | ref 6 | this work | ref 37 | ref 17 |
| $A_{1g}$ | 587 | 584 | 323 | 327 | 327 | 213 | 219 | |
| $B_{1g}$ | 383 | 330 | 184 | 188 | 188 | 106 | 139 | 133<br>124 sh |
| $B_{2g}$ | 603-590[c] | 530 | 327-324[c] | 319? | (255)[d] | (~214)[e] | (219)[e] | |
| $E_u$ | 542 | 460 | 302 | 306 | 306 | 187 | | |

[a] *Average* data for each species are given. [b] Data for $Se_4(AlCl_4)_2$ is not included in this table. [c] Range of observed values. [d] Calculated by normal-coordinate methods; see text. [e] Estimated values.

split $E_u$ mode. Generally the $E_u$ band, or this band when it is split under the site or factor group symmetry of the cation in any particular compound,[34] appears only weakly in the Raman spectra of compounds of the $Se_4^{2+}$ species. In $Se_4(AlCl_4)_2$, if this latter assignment were used, the high-frequency component (298 $cm^{-1}$) would then have been disproportionately strong. (Note that the presumed low-frequency component at 289 $cm^{-1}$ does exhibit only a "normal" weak intensity.) In fact, the band at 298 $cm^{-1}$ (301 $cm^{-1}$ at −196 °C) has a relative intensity that is very similar to that of the $B_{2g}$ mode in $Se_4(HS_2O_7)_2$, and moreover, the $A_{1g}$ mode in $Se_4(AlCl_4)_2$ shows no evidence for any asymmetry (Figure 2), although this could merely indicate that the $B_{2g}$ and $A_{1g}$ modes are coincident. However, the Raman data do suggest that a weak band appears as a shoulder slightly to higher frequencies than the peak at 298 $cm^{-1}$. This band (ca. 303 $cm^{-1}$) and the one at 298 $cm^{-1}$ both appear in the infrared spectrum while the one at 298 $cm^{-1}$ does not, so that for this reason and the ones given above, the peak at 298 $cm^{-1}$ is assigned as the $B_{2g}$ mode and the two weak peaks at ca. 303 and 289 $cm^{-1}$ as a split $E_u$ mode. Notably, this was the only example found in this study where the $B_{2g}$ mode has a lower frequency than the $A_{1g}$ mode. It is also interesting that the $A_{1g}$ mode in $Se_4(AlCl_4)_2$ is ca. 10–14 $cm^{-1}$ lower than the $A_{1g}$ mode in all other compounds of $Se_4^{2+}$ that have been examined. If the above assignment is correct, then, together with the somewhat anomalous $A_{1g}$ frequency, this presumably reflects a very different interaction of the $Se_4^{2+}$ cations with the environment created by the $AlCl_4^-$ anions compared with interactions in other compounds, particularly $Se_4(HS_2O_7)_2$. This is also apparent, as pointed out above, from a consideration of the corresponding electronic diffuse-reflectance spectra. Somewhat surprisingly, however, there is no evidence for a similar manifestation in the vibrational data of the appropriate $Te_4^{2+}$ salts, although in view of the smaller differences expected between the $B_{2g}$ and $A_{1g}$ modes in $Te_4^{2+}$ compared to those in $Se_4^{2+}$ (in turn smaller than those in $S_4^{2+}$), the modes may not be resolvable. Indeed, the "$A_{1g}$" modes in the Raman spectra of compounds of $Te_4^{2+}$ do appear somewhat asymmetric.

Previously, in their studies on the $Se_4^{2+}$ species, Gillespie and Pez[5] observed a band at 319 $cm^{-1}$ in $Se_4(SO_3F)_2$, slightly to *lower* frequencies than the intense $A_{1g}$ mode (327 $cm^{-1}$ in their work), which they suggested was the $B_{2g}$ mode. The position of this band was not inconsistent with the value calculated by normal-coordinate methods (306 $cm^{-1}$). This band was observed only in $Se_4(SO_3F)_2$ and not in any of the other compounds studied. Steudel,[6] on the other hand, suggested that the band at 319 $cm^{-1}$ was somewhat high for the $B_{2g}$ mode on the basis of calculations using Urey–Bradley force constants transferred from cyclooctaselenium, $Se_8$. Accordingly, Steudel used the observed data for the $A_{1g}$, $B_{1g}$, and $E_u$ modes for $Se_4^{2+}$ together with a Urey–Bradley bond–bond interaction force constant transferred from $Se_8$ to calculate a frequency for the $B_{2g}$ mode. This value was 255 $cm^{-1}$. It was concluded that the $B_{2g}$ mode was probably of low Raman intensity and, as such, had yet to be observed. Steudel also attributed the band at 319 $cm^{-1}$ in $Se_4(SO_3F)_2$ to a "factor-group" splitting of the $A_{1g}$ mode.

Chart I

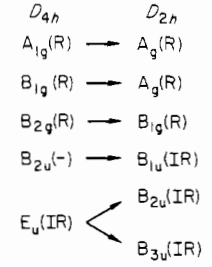


On the basis of the present studies on the $S_4^{2+}$, $Se_4^{2+}$, and $Te_4^{2+}$ cations it is apparent that the $B_{2g}$ mode is found quite close to the $A_{1g}$ mode and generally to higher frequencies than the latter. An exception to this would appear to be $Se_4(AlCl_4)_2$, and perhaps $Se_4(SO_3F)_2$, where the ordering of these modes is reversed. The difference in frequency between the $A_{1g}$ and $B_{2g}$ modes also appears to be highly dependent on the nature, number of interactions, and orientation of the counteranions in the particular compound (for charge transfer, interactions within the plane of the cation are probably important). Indeed, this difference appears to increase as the cation–anion interactions increase in strength and the bond distance in the cation becomes larger; i.e., there is an increase in covalency. This is evident from the data on $Se_4^{2+}$, as presented above. For $S_4^{2+}$ the spectroscopic and crystallographic data are not as extensive, but the S–S bond in $S_4(AsF_6)_2 \cdot 0.6SO_2$ is 2.014 (4) Å, slightly longer than that in $(S_4^{2+})(S_7I^+)_4(AsF_6^-)_6$, which has a length of 1.98 (1) Å.[35] Significantly, the former compound has more (and shorter) close cation–anion contacts (less than the sum of the appropriate van der Waals distances) than the latter,[18] suggesting some covalent character, as well as exhibiting a rather large difference (17 $cm^{-1}$) between the $B_{2g}$ and $A_{1g}$ modes for an $S_4^{2+}$ salt (see above). Data for $Te_4^{2+}$ appear less conclusive, for although there are significant differences between the Te–Te bond distances in $Te_4(Al_2Cl_7)_2$, 2.660 (2) Å,[36] $Te_4(AlCl_4)_2$, 2.669 (2) Å,[36] and $Te_4(SbF_6)_2$, 2.673 (3) Å (average value),[18] the difference between the $B_{2g}$ and $A_{1g}$ modes is much less for $Te_4^{2+}$ (ca. 1–2 $cm^{-1}$) than for $S_4^{2+}$ and $Se_4^{2+}$ and precludes correlations of this type.

A summary of the present data for the $S_4^{2+}$, $Se_4^{2+}$, and $Te_4^{2+}$ cations is given in Table VI, together with previous assignments for these three cations. Considerable differences between the

(34) The site symmetry of the $Se_4^{2+}$ cation in $Se_4(HS_2O_7)_2$, $Se_4(Sb_2F_4)(Sb_2F_5)(SbF_6)_5$, and $Se_4(AlCl_4)_2$ is $C_i$ in the first two and $C_{2h}$ in the last so that further treatment is warranted. See also ref 5.

(35) Passmore, J.; Sutherland, G.; White, P. S. *J. Chem. Soc., Chem. Commun.* **1980**, 330.
(36) Couch, T. W.; Lokken, D. A.; Corbett, J. D. *Inorg. Chem.* **1972**, *11*, 357.
(37) Barr, J.; Gillespie, R. J.; Kapoor, R.; Pez, G. P. *J. Am. Chem. Soc.* **1968**, *90*, 6855.

**Table VII.** Vibrational Data ($cm^{-1}$) for *trans*-$Te_2Se_2^{2+}$ in *trans*-$Te_2Se_2^{2+}(Sb_3F_{14}^-)(SbF_6^-)$[a,b]

| Raman | | | |
|---|---|---|---|
| soln (65% oleum) | solid | IR | assignt |
| 267 (100) pol | 268 (100) | | $\nu_1(A_g)$, $\nu_3(B_{1g})$ |
| | | 253 sh[c] | $\nu_5(B_{2u})$ |
| | | 242 | $\nu_6(B_{3u})$ |
| 139 (15) pol | 139 (9) | | $\nu_2(A_g)$ |
| | | 115 or 80 or 69 | $\nu_4(B_{1u})$? |

[a] Spectra recorded at room temperature. [b] Raman intensities in parentheses. [c] Shoulder on very strong Sb–F stretch at 280 $cm^{-1}$.

assignments for $S_4^{2+}$ and $Te_4^{2+}$ are noted, while those for $Se_4^{2+}$ are substantially as reported by Gillespie and Pez.[5]

**The *trans*-$Te_2Se_2^{2+}$ Cation.** On reduction in symmetry of an isolated square-planar cation from $D_{4h}$ to $D_{2h}$ the correlations shown in Chart I occur.[38] We note that there are now two totally symmetric vibrations, the $E_u$ mode splits, and that the inactive $B_{2u}$ mode becomes the infrared-active $B_{1u}$ mode under $D_{2h}$ symmetry. As the $D_{2h}$ point group still has a center of inversion, the mutual exclusion rule also applies.

The vibrational data for the *trans*-$Te_2Se_2^{2+}$ cation in *trans*-$Te_2Se_2^{2+}(Sb_3F_{14}^-)(SbF_6^-)$ are given in Table VII. Polarization measurements in solution confirmed the identity of the two $A_g$ modes, which fall about midway between the corresponding values for the $Se_4^{2+}$ and $Te_4^{2+}$ cations, as expected. However, in neither the solution nor solid-state Raman spectra was there any evidence for a separate $B_{1g}$ mode (the $B_{2g}$ mode under $D_{4h}$ symmetry), and it is assumed that, under the limits of resolution (2 $cm^{-1}$) in recording the spectrum, this mode is almost coincident with the high-frequency $A_g$ ($A_{1g}$ under $D_{4h}$ symmetry) mode, as for $D_{4h}$ molecules. The infrared-active but Raman-inactive $B_{2u}$ and $B_{3u}$ modes were easily identified from a consideration of Raman and infrared coincidences as well as comparison with the vibrational data for $(S_4N_4^{2+})(Sb_3F_{14}^-)(SbF_6^-)$,[39] which contains the same two anions. However, the same approach was not as successful in the identification of the out-of-plane $B_{1u}$ mode as in this case there remained a choice between three peaks: one rather strong peak at 115 $cm^{-1}$ and two weaker peaks at 80 and 69 $cm^{-1}$. As all of these fall in the region of lattice vibrations, it is not possible to say which, if any, is the $B_{1u}$ mode, although the peak at 115 $cm^{-1}$ is probably too high for the out-of-plane $B_{1u}$ mode.

**Vibrational Analysis.** The assignments for the Raman- and infrared-active bands of the $S_4^{2+}$, $Se_4^{2+}$, $Te_4^{2+}$, and *trans*-$Te_2Se_2^{2+}$ cations have been discussed above, on the basis of square-planar structures with either $D_{4h}$ or $D_{2h}$ point group symmetry, where appropriate.

The G and F matrices (for both $D_{4h}$ and $D_{2h}$ symmetry) were constructed according to the methods described by Wilson, Decius, and Cross,[38] using the programs EXCART, GBMMOD, and FGZSYM.[40] In view of the variations in the bond lengths and differences in the frequencies of the normal modes of vibration from compound to compound, as well as the approximate nature of the potential field (see below), only average values for each species were employed. Thus S–S, Se–Se, Te–Te, and Te–Se bond distances (directly bonded) were set at 2.000, 2.275, 2.672, and 2.476 Å, respectively, while the vibrational data used were listed in Tables VI and VII.

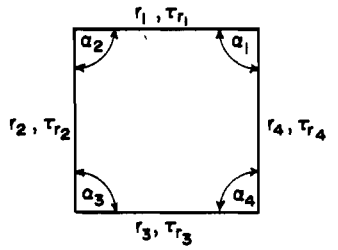


**Figure 3.** Geometry and arrangement of the internal coordinates for a square-planar system ($D_{4h}$); $r_0$ is the equilibrium chalcogen–chalcogen distance, and $\alpha$ is the equilibrium interbond angle (=90°).

**Table VIII.** Symmetry Coordinates for Square-Planar $D_{4h}$ and $D_{2h}$ Systems[a]

Symmetry Coordinates

| $D_{4h}$ ($D_{2h}$) | |
|---|---|
| $A_{1g}$ ($A_g$) | $S = 1/2(r_1 + r_2 + r_3 + r_4)$ |
| $B_{1g}$ ($A_g$) | $S = (r_0/2)(\alpha_1 - \alpha_2 + \alpha_3 - \alpha_4)$ |
| $B_{2g}$ ($B_{1g}$) | $S = 1/2(r_1 - r_2 + r_3 - r_4)$ |
| $B_{2u}$ ($B_{1u}$) | $S = (r_0/2)(\tau_1 - \tau_2 + \tau_3 - \tau_4)$ |
| $E_u$ ($B_{2u}$) | $S_a = (1/12^{1/2})(r_1 - r_2 - r_3 + r_4) - (r_0/3^{1/2})(\alpha_1 - \alpha_3)$ |
| $E_u$ ($B_{3u}$) | $S_b = (1/12^{1/2})(r_1 + r_2 - r_3 - r_4) - (r_0/3^{1/2})(\alpha_2 - \alpha_4)$ |

Redundancy Conditions

| $D_{4h}$ ($D_{2h}$) | |
|---|---|
| $A_{1g}$ ($A_g$) | $(r_0/2)(\alpha_1 + \alpha_2 + \alpha_3 + \alpha_4) \equiv 0$ |
| $A_{1u}$ ($A_u$) | $(r_0/2)(\tau_1 + \tau_2 + \tau_3 + \tau_4) \equiv 0$ |
| $E_g$ ($B_{2g}$) | $(r_0/2^{1/2})(\tau_1 - \tau_3) \equiv 0$ |
| $E_g$ ($B_{3g}$) | $(r_0/2^{1/2})(\tau_2 - \tau_4) \equiv 0$ |
| $E_u$ ($B_{2u}$) | $(1/6^{1/2})(r_1 - r_2 - r_3 + r_4) + (r_0/6^{1/2})(\alpha_1 - \alpha_3) \equiv 0$ |
| $E_u$ ($B_{3u}$) | $(1/6^{1/2})(r_1 + r_2 - r_3 - r_4) + (r_0/6^{1/2})(\alpha_2 - \alpha_4) \equiv 0$ |

[a] The symmetry coordinates for $D_{2h}$ may be obtained from $D_{4h}$ by following the permutation $r_1 \rightarrow r_1$, $r_2 \rightarrow d_1$, $r_3 \rightarrow r_2$, and $r_4 \rightarrow d_2$ and similarly for $\alpha_i$ ($\rightarrow \alpha_i$ or $\beta_i$) and $\tau_{r_i}$ ($\rightarrow \tau_{r_i}$ or $\tau_{d_i}$).

The internal coordinates chosen were changes in the bond distances, internal angles at each atom, and torsional coordinates around each bond. These are illustrated in Figure 3. The symmetry coordinates constructed from these internal coordinates, listed in Table VIII, were used in the program FGZSYM to symmetrize the G and F matrices.

For a square-planar structure with $D_{4h}$ symmetry, the generalized valence force field (GVFF) requires 3 primary and 13 interaction force constants, and may be expressed as

$$2V = f_r\sum^{4}\Delta r_{ij}^2 + r^2f_\alpha\sum^{4}\Delta\alpha_{ijk}^2 + r^2f_\tau\sum^{4}\Delta\tau_{ij}^2 + 2f_{rr}\sum^{4}\Delta r_{ij}\Delta r_{jk} + 2f_{rr}'\sum^{2}\Delta r_{ij}\Delta r_{kl} + 2r^2f_{\alpha\alpha}\sum^{4}\Delta\alpha_{ijk}\Delta\alpha_{jkl} + 2r^2f_{\alpha\alpha}'\sum^{2}\Delta\alpha_{ijk}\Delta\alpha_{ikl} + 2r^2f_{\tau\tau}\sum^{4}\Delta\tau_{ij}\Delta\tau_{jk} + 2r^2f_{\tau\tau}'\sum^{2}\Delta\tau_{ij}\Delta\tau_{kl} + 2rf_{r\alpha}\sum^{8}\Delta r_{ij}\Delta\alpha_{ijk} + 2rf_{r\alpha}'\sum^{8}\Delta r_{ij}\Delta\alpha_{jkl} + 2rf_{r\tau}\sum^{4}\Delta r_{ij}\Delta\tau_{ij} + 2rf_{r\tau}'\sum^{8}\Delta r_{ij}\Delta\tau_{jk} + 2rf_{r\tau}''\sum^{4}\Delta r_{ij}\Delta\tau_{kl} + 2r^2f_{\alpha\tau}\sum^{8}\Delta\alpha_{ijk}\Delta\tau_{ij} + 2r^2f_{\alpha\tau}'\sum^{8}\Delta\alpha_{ijk}\Delta\tau_{kl}$$

where $\Delta r_{ij}$, $\Delta\alpha_{ijk}$, and $\Delta\tau_{ij}$ represent changes in the equilibrium positional, angle, or torsional coordinates of the relevant atoms, respectively, and the force constants are defined in Table IX. In the case of a system with $D_{2h}$ symmetry, the potential field is an expanded version of the above because of the loss in symmetry, with 4 (unique) primary and 21 (unique) interaction force constants. For the model with $D_{4h}$ symmetry, the

(38) Wilson, E. B.; Decius, J. C.; Cross, P. C. "Molecular Vibrations"; McGraw-Hill: New York, 1955.
(39) Tyrer, J. D. Ph.D. Thesis, McMaster University, 1979.
(40) The computer programs GBMMOD, FGZSYM, and GFPP were written by J. H. Schactschneider, Technical Report No. 9032-VII, 1965, of the Shell Development Co. and modified by W. V. F. Brooks in 1968, then at Ohio University, now at the University of New Brunswick. The above programs, and EXCART, were obtained from H. F. Shurvell of Queen's University and modified to run on a CDC 6400 computer.

**Table IX.** Valence Force Constants (mdyn/Å) for the $S_4^{2+}$, $Se_4^{2+}$, $Te_4^{2+}$, and *trans*-$Te_2Se_2^{2+}$ Polyatomic Cations[a,b]

| force constant | $S_4^{2+}$ | $Se_4^{2+}$ [c] | $Te_4^{2+}$ |
|---|---|---|---|
| $f_r$ | 2.690 | 2.086 (1.905) | 1.408 |
| $f_\alpha$ | 0.345 | 0.197 (0.188) | 0.106 |
| $f_{rr}$ | −0.048 to −0.014[d] | −0.015 to −0.004[d] (0.050) | −0.004 |
| $f_{rr}'$ | 0.615 | 0.359 (0.259) | 0.305 |

| force constant[b] | *trans*-$Te_2Se_2^{2+}$ A | B | force constant[b] | *trans*-$Te_2Se_2^{2+}$ A | B |
|---|---|---|---|---|---|
| $f_r$ | 1.781 | 1.781 | $f_{rr(Se)}$ | −0.008 | −0.010 |
| $f_{\alpha(Se)}$ | 0.178 | 0.180 | $f_{rr(Te)}$ | −0.008 | −0.005 |
| $f_{\beta(Te)}$ | 0.100 | 0.097 | $f_{rr}'$ | 0.298 | 0.298 |

[a] Definitions: $f_r$, chalcogen-chalcogen stretch; $f_\alpha$, interbond angle bend; $f_{rr}$, stretch-stretch interaction (adjacent); $f_{rr}'$, stretch-stretch interaction (opposite); $f_{\alpha\alpha}$, angle bend-angle bend interaction (adjacent); $f_{\alpha\alpha}'$, angle bend-angle bend interaction (opposite); $f_{r\alpha}$, stretch-angle bend interaction (bond in common); $f_{r\alpha}'$, stretch-angle bend interaction (no bond in common); $f_\tau$, torsion; $f_{\tau\tau}$, torsion-torsion interaction (adjacent); $f_{\tau\tau}'$, torsion-torsion interaction (opposite); $f_{r\tau}$, stretch-torsion interaction (torsion around bond); $f_{r\tau}'$, stretch-torsion interaction (one atom in common); $f_{r\tau}''$, stretch-torsion interaction (no atom in common); $f_{\alpha\tau}$, angle bend-torsion interaction (one bond in common); $f_{\alpha\tau}'$, angle bend-torsion interaction (no bond in common). [b] See ref 41 for definitions of these valence force constants. [c] Data for $Se_4(AlCl_4)_2$ given in parentheses. [d] Range of values.

**Table X.** G and F Matrix Elements for a Square-Planar ($D_{4h}$) System

| species | G element[a] | F element |
|---|---|---|
| $A_{1g}$ | $2\mu$ | $F_{A_{1g}} = f_r + 2f_{rr} + f_{rr}'$ |
| $B_{1g}$ | $8\mu$ | $F_{B_{1g}} = f_\alpha - 2f_{\alpha\alpha} + f_{\alpha\alpha}'$ |
| $B_{2g}$ | $2\mu$ | $F_{B_{2g}} = f_r - 2f_{rr} + f_{rr}'$ |
| $B_{2u}$ | $16\mu$ | $F_{B_{2u}} = f_\tau - 2f_{\tau\tau} + f_{\tau\tau}'$ |
| $E_u$ | $6\mu$ | $F_{E_u} = {}^1/_3(f_r - f_{rr} - 4f_{r\alpha} + 4f_{r\alpha}' + 2f_\alpha - 2f_{\alpha\alpha}')$ |

[a] $\mu$ represents the inverse mass of the particular atom.

resulting (symmetrized) G and F matrix elements obtained after diagonalization are given in Table X, and it may be noted that the number of valence force constants has been reduced by five (the interaction force constants between in-plane and out-of-plane coordinates). A similar reduction (eight interaction force constants) occurs under $D_{2h}$ symmetry. However, in either case there are still too many force constants to be evaluated from the observed vibrational data, so that a number of modifications were made to the respective potential fields. This entailed restricting all interaction force constants other than bond–bond stretching interactions to zero. If the out-of-plane vibrations are neglected for the moment, then in the $D_{4h}$ model this allows $f_r$, $f_\alpha$, $f_{rr}$, and $f_{rr}'$ to be estimated, but under $D_{2h}$ symmetry there is still one more force constant (viz., $f_r$, $f_{\alpha(Se)}$, $f_{\beta(Te)}$, $f_{rr(Se)}$, $f_{rr(Te)}$, and $f_{rr}'$[41]) than the number of vibrational data. (The $B_{1g}$ mode was assumed to lie 2 $cm^{-1}$ to higher frequencies than the $A_g$ mode at 268 $cm^{-1}$.) For the $D_{2h}$ model two approximations were subsequently used, one with $f_{rr(Se)} = f_{rr(Te)}$ (A) and the other with $f_{rr(Se)} = 2f_{rr(Te)}$ (B), the latter scaling based on the average values of the related force constants found for $Se_4^{2+}$ and $Te_4^{2+}$. Solution of the secular equation was carried out by computer using the program GFPP[40] until complete agreement between observed and calculated frequencies was obtained, and the results are listed in Table IX, while the respective potential energy distributions are given in Table XI. It may be noted that there is very little difference between the two potential fields for *trans*-$Te_2Se_2^{2+}$, with variations between $f_{rr(Se)}$ and $f_{rr(Te)}$ causing only very slight changes in the primary force constants $f_{\alpha(Se)}$ and $f_{\beta(Te)}$.

**Table XI.** Potential Energy Distributions for the $S_4^{2+}$, $Se_4^{2+}$, $Te_4^{2+}$, and *trans*-$Te_2Se_2^{2+}$ Polyatomic Cations

$S_4^{2+}$, $Se_4^{2+}$, $Te_4^{2+}$ [a,b]

| species | cation | $V_r$ | $V_\alpha$ | $V_{rr}$ | $V_{rr}'$ |
|---|---|---|---|---|---|
| $A_{1g}$ | $S_4^{2+}$ | 83 | 0 | −2 | 19 |
| | $Se_4^{2+}$ | 86 (84) | 0 (0) | −1 (4) | 15 (12) |
| | $Te_4^{2+}$ | 83 | 0 | −1 | 18 |
| $B_{1g}$ | $S_4^{2+}$ | 0 | 100 | 0 | 0 |
| | $Se_4^{2+}$ | 0 (0) | 100 (100) | 0 (0) | 0 (0) |
| | $Te_4^{2+}$ | 0 | 100 | 0 | 0 |
| $B_{2g}$ | $S_4^{2+}$ | 80 | 0 | 2 | 18 |
| | $Se_4^{2+}$ | 85 (92) | 0 (0) | 1 (−5) | 14 (13) |
| | $Te_4^{2+}$ | 82 | 0 | 1 | 17 |
| $E_u$ | $S_4^{2+}$ | 97 | 25 | 0 | −22 |
| | $Se_4^{2+}$ | 98 (94) | 19 (19) | 0 (0) | −17 (−13) |
| | $Te_4^{2+}$ | 107 | 16 | 0 | −23 |

*trans*-$Te_2Se_2^{2+}$

| species | freq, $cm^{-1}$ | pot. field | $V_r$ | $V_{\alpha(Se)}$ | $V_{\beta(Te)}$ | $V_{rr(Se)}$ | $V_{rr(Te)}$ | $V_{rr}'$ |
|---|---|---|---|---|---|---|---|---|
| $A_g$ | 268 | A | 86.3 | 0 | 0 | −0.4 | −0.4 | 14.4 |
| | | B | 86.3 | 0 | 0 | −0.5 | −0.3 | 14.4 |
| $A_g$ | 139 | A | 0 | 64.1 | 35.9 | 0 | 0 | 0 |
| | | B | 0 | 64.9 | 35.1 | 0 | 0 | 0 |
| $B_{1g}$ | 270 | A | 85.0 | 0 | 0 | 0.4 | 0.4 | 14.2 |
| | | B | 85.0 | 0 | 0 | 0.5 | 0.3 | 14.2 |
| $B_{2u}$ | 253 | A | 96.9 | 19.3 | 0 | −0.4 | 0.4 | −16.2 |
| | | B | 96.9 | 19.6 | 0 | −0.5 | 0.3 | −16.2 |
| $B_{3u}$ | 242 | A | 105.9 | 0 | 11.8 | 0.5 | −0.5 | −17.7 |
| | | B | 105.9 | 0 | 11.6 | 0.6 | −0.3 | −17.7 |

[a] Average values. [b] Data for $Se_4(AlCl_4)_2$ given in parentheses.

Comparison of the force constant data obtained in this study is best made with that of other homopolyatomic species that have cumulated chalcogen–chalcogen single bonds such as $S_6$, $S_{12}$, and $Se_8$. These data are listed in Table XII, together with data for other species that also have chalcogen–chalcogen single bonds. However, the latter species are less appropriate for comparative purposes because of the heteroatoms which flank only one chalcogen–chalcogen bond in each case. Furthermore, the chalcogen–chalcogen bond distances in several of these species are presently unknown.

In general, the bond stretching force constants for $S_4^{2+}$ and $Se_4^{2+}$ are significantly greater than those given in Table XII. This is consistent with the formal (valence bond) bond order of 1.25 for all three $M_4^{2+}$ cations. Data on tellurium species are not as extensive (only $Te_6^{4+}$, a cluster cation, is listed above), but for $(CH_3)_2Te_2$[50] (Te–Te = 2.70 Å, assumed value) both the Te–Te stretching frequency (188 $cm^{-1}$) and the (symmetrized) Te–Te stretching force constant (1.424

(41) For a *trans*-$Te_2Se_2^{2+}$ system of $D_{2h}$ symmetry, the force constants remaining after introduction of the above approximations into the potential field are defined as follows: $f_r$, Te–Se stretch; $f_{\alpha(Se)}$, interbond angle bend at Se; $f_{\beta(Te)}$, interbond angle bend at Te; $f_{rr(Se)}$, interaction between two adjacent bond stretches with a Se atom in common; $f_{rr(Te)}$, interaction between two adjacent bonds stretches with a Te atom in common; $f_{rr}'$, interaction between two bond stretches that occur opposite each other.

(42) Nimon, L. A.; Neff, V. D. *J. Mol. Spectrosc.* **1968**, *26*, 175.
(43) Scott, D. W.; McCullough, J. P.; Kruse, F. H. *J. Mol. Spectrosc.* **1964**, *13*, 313.
(44) Steudel, R.; Eggers, D. F., Jr. *Spectrochim. Acta, Part A* **1975**, *31A*, 879.
(45) Winnewisser, B. P.; Winnewisser, M. *Z. Naturforsch., A* **1968**, *23A*, 832.
(46) Fonneris, R.; Hennies, C. E. *J. Mol. Struct.* **1970**, *5*, 449.
(47) Scott, D. W.; Finke, H. L.; Gross, M. E.; Guthrie, G. B.; Huffman, H. M. *J. Am. Chem. Soc.* **1950**, *72*, 2424.
(48) Scott, D. W.; El-Sabban, M. Z. *J. Mol. Spectrosc.* **1969**, *31*, 362.
(49) Burns, R. C.; Gillespie, R. J. *Spectrochim. Acta*, in press.
(50) Sink, C. W.; Harvey, A. B. *J. Mol. Struct.* **1969**, *4*, 203.

**Table XII.** Selected Valence Force Constants for Species Containing Chalcogen–Chalcogen Single Bonds and for Related Molecules[a]

| species | Ch–Ch, Å | $f_r$ | $f_\alpha$ | $f_{rr}$[b] | $f_{rr'}$[c] | $f_\tau$ | ref |
|---|---|---|---|---|---|---|---|
| $S_6$[d] | 2.057 | 2.230 | 0.228 | 0.530 | −0.003 | 0.046 | 42 |
| $S_8$[e] | 2.047 | 2.366 | 0.234 | 0.612 | 0.041 | 0.040 | 43 |
| $S_{12}$[e] | 2.053 | 2.367 | 0.261 | 0.584 | 0.018 | 0.028 | 44 |
| $H_2S_2$[d] | 2.055 | 2.52–2.62[g] | | | | | 45 |
| $S_2Cl_2$[d] | 1.97 | 2.610 | | | | | 46 |
| $S_2Br_2$[d] | 1.97 | 2.500 | | | | | 46 |
| $(CH_3)_2S_2$[d] | 2.04[f] | 2.55, 3.096 | | | | | 47, 48 |
| $Se_8$[e] | 2.336 | 1.695 | 0.166 | 0.394 | 0.037 | 0.030 | 6 |
| $Se_2Cl_2$[d] | 2.28[f] | 1.880 | | | | | 46 |
| $Se_2Br_2$[d] | 2.28[f] | 1.740 | | | | | 46 |
| $Te_6^{4+}$[d] | 2.675[h] | 1.129 | | | | | 49 |
| | 3.133[i] | 0.635–0.934[g] | | | | | |

[a] Force constants in mdyn/Å. [b] Interaction with nearest neighbor. [c] Interaction with next-nearest neighbor. [d] Modified valence force field. [e] Modified Urey–Bradley force field. [f] Assumed value. [g] Range dependent on choice of interaction force constants. [h] Te–Te bonds in triangular faces of trigonal prism. [i] Long Te–Te bonds between triangular faces of trigonal prism.

**Table XIII.** Symmetry Coordinates (for Central Force Coordinates) for the In-Plane Motions of a Square-Planar System with $D_{4h}$ Symmetry

Symmetry Coordinates

$$A_{1g}:\ S = (1/2(2^{1/2}))(d_1 + d_2 + d_3 + d_4) + {}^1/_2(D_1 + D_2)$$
$$B_{1g}:\ S = (1/2^{1/2})(D_1 - D_2)$$
$$B_{2g}:\ S = {}^1/_2(d_1 - d_2 + d_3 - d_4)$$
$$E_u:\ S_a = (1/2^{1/2})(d_1 - d_3)$$
$$S_b = (1/2^{1/2})(d_2 - d_4)$$

Redundancy

$$A_{1g}:\ (1/2(2^{1/2}))(d_1 + d_2 + d_3 + d_4) - {}^1/_2(D_1 + D_2) \equiv 0$$

mdyn/Å, VFF) are lower than the corresponding values for $Te_4^{2+}$ ($A_{1g}$ mode: 213 $cm^{-1}$ and 1.705 mdyn/Å). For $S_4^{2+}$ and $Se_4^{2+}$ values for the other force constants are quite similar to those found in species that have cumulated chalcogen–chalcogen bonds. Note, however, that the magnitudes of $f_{rr}$ and $f_{rr}'$ are reversed relative to those in these other compounds; the small values of $f_{rr}$ in the case of the square-planar species are not unexpected, as one might anticipate little interaction between two bonds at 90°, particularly in view of the high p-orbital contributions to the bonding in the cations.[26] No data have previously been reported on systems that have Te–Se bonds, but the values obtained for *trans*-$Te_2Se_2^{2+}$ are, not unexpectedly, intermediate between those for $Se_4^{2+}$ and $Te_4^{2+}$ or, for $f_{\alpha(Se)}$ and $f_{\beta(Te)}$, very similar to the values obtained for the respective homopolyatomic species themselves.

Of the four force constants that have been calculated in the $D_{4h}$ system, only $f_{rr}$ can be identically evaluated as it is independent of approximations in the potential field. This interaction force constant may be obtained from those parts of the secular equation that deal with the $A_{1g}$ and $B_{2g}$ species (Table X). As the $B_{2g}$ mode generally appears to higher frequencies than the $A_{1g}$ mode, as shown above, this force constant is negative in sign and varies in magnitude as the difference in frequency between the $A_{1g}$ and $B_{2g}$ modes varies. However, in $Se_4(AlCl_4)_2$ the $B_{2g}$ mode was assigned at a *lower* frequency than the $A_{1g}$ mode, which results in a change in sign of the $f_{rr}$ interaction force constant. Data for $Se_4(AlCl_4)_2$, with the same approximations in the potential field as described above, are also reported in Tables IX and XI. It is noted that the value for $f_r$ (1.905 mdyn/Å) is somewhat less than the average for $Se_4^{2+}$, although it is still greater than the other Se–Se stretching force constants given in Table XII. The reduced value of $f_r$ is caused both by the change in sign of $f_{rr}$ and by the shift to lower frequencies of the $A_{1g}$ mode relative to those in other salts of the $Se_4^{2+}$ cation. Although it is not certain how the approximations introduced into the potential field will affect $f_r$, the somewhat reduced value of this force constant for $Se_4(AlCl_4)_2$ is consistent with the rather long Se–Se bond distances in this compound.

In the above discussion, no comparisons have been made concerning the out-of-plane (ring puckering) $B_{2u}$ or $B_{1u}$ modes for any of the cations. Unfortunately, under $D_{4h}$ symmetry the $B_{2u}$ mode is neither Raman nor infrared active, whereas under $D_{2h}$ symmetry the $B_{1u}$ mode is infrared active. However, no definite assignment could be made for *trans*-$Te_2Se_2^{2+}$, as previously indicated. We can, nevertheless, make some estimate of where these modes will occur with the data in hand. In the vibrational treatment the out-of-plane mode is described in terms of torsional internal coordinates. Examination of the data in Table XII indicates that, for sulfur species, $f_\tau$ increases as the ring size decreases. This is consistent with a decrease in flexibility with a decrease in ring size. For $S_4^{2+}$, $f_\tau$ would therefore be expected to be slightly larger than for $S_6$, ~0.050 mdyn/Å. Similarly, $f_\tau$ for $Se_4^{2+}$ and $Te_4^{2+}$ are estimated to be about 0.035 and 0.020 mdyn/Å, respectively. With the assumption that $f_{\tau\tau}$ and $f_{\tau\tau}'$ (Table X) are both zero, the $B_{2u}$ modes are calculated at 206, 110, and 65 $cm^{-1}$ for $S_4^{2+}$, $Se_4^{2+}$, and $Te_4^{2+}$, respectively. As $f_{\tau\tau}$ and $f_{\tau\tau}'$ are probably significant, these represent upper limits to the frequencies at which the modes are likely to be found. Indeed, Steudel[6] calculated a frequency of 73 $cm^{-1}$ for the $B_{2u}$ mode in $Se_4^{2+}$ using a Urey–Bradley force constant transferred from $Se_8$.

Recently, Bartell and co-workers[8] derived (theoretically) symmetrized force constants and vibrational frequencies for $Te_4^{2+}$ using an ab initio pseudopotential MO method. In general their force constants, and hence vibrational frequencies, are considerably greater than the above experimental values,[51] with $\nu_1(A_{1g})$ = 251, $\nu_2(B_{1g})$ = 137, $\nu_3(B_{2g})$ = 322, $\nu_4(B_{2u})$ = 45, and $\nu_5(E_u)$ = 268 $cm^{-1}$. Interestingly, the $B_{2g}$ mode is predicted to appear at higher frequencies than the $A_{1g}$ mode, but so too is the $E_u$ mode. The latter ordering was not observed for any of the cations in the present work. The calculated value of the out-of-plane $B_{2u}$ mode, 45 $cm^{-1}$, is a little less than our estimate of 65 $cm^{-1}$. If, like the other theoretically calculated vibrational frequencies, the $B_{2u}$ frequency has been overestimated, then our value is probably much higher than is realistic and suggests that the interaction force constants, $f_{\tau\tau}$ and $f_{\tau\tau}'$, are not significant in this case. For the related *trans*-$Te_2Se_2^{2+}$ cation, therefore, the $B_{1u}$ vibration is likely to occur at about 50–70 $cm^{-1}$, so that the peak at 69 $cm^{-1}$ is tentatively assigned as this mode.

**Acknowledgment.** We thank the Natural Sciences and Engineering Research Council of Canada for financial support of this work; we also thank Mr. Jan Monster of Nuclear

(51) It should be noted that the general reliability of the pseudopotential method for the calculation of force fields (and hence vibrational frequencies) has yet to be established, especially for ions. Calculations on the lower fluorides of iodine and xenon have given vibrational frequencies correct to only 10–20%.[8]

Chemistry, McMaster University, for providing the sample of $Ag_2S$ enriched in $^{34}S$, Dr. J. Vekris and M. Collins for providing some of the samples, and B. Christian for obtaining preliminary diffuse-reflectance measurements.

## Appendix

Although they are not conventionally used, it is possible to describe the vibrational motion (in this case the in-plane motion) of a square-planar $D_{4h}$ system in terms of central force coordinates. Teranishi and Decius[52] treated a planar $XY_3$ system in this manner, while Cyvin[4,53] has dealt with the nonlinear $XY_2$, tetrahedral $XY_4$, and octahedral $XY_6$ systems. Generally, treatment of the vibrational problem by central force coordinates leads to simpler **G** matrices and simpler expressions for the normal frequencies and may be of use in the study of mean-square amplitudes of vibration because of the mean amplitudes of nonbonded pairs.[4,52]

The internal coordinates used in this case are simply the changes in the directly bonded ($\Delta d_i$) and nonbonded (diagonal) distances ($\Delta D_i$). The resulting symmetry coordinates constructed from these internal coordinates are given in Table XIII. For a $D_{4h}$ system, the generalized (central) force field is expressed as

$$2V = f_d\sum^{4}\Delta d_{ij}^2 + f_D\sum^{2}\Delta D_{ij}^2 + 2f_{dd}\sum^{4}\Delta d_{ij}\Delta d_{jk} + 2f_{dd}'\sum^{2}\Delta d_{ij}\Delta d_{kl} + 2f_{DD}\sum^{1}\Delta D_{ij}\Delta D_{kl} + 2f_{dD}\sum^{8}\Delta d_{ij}\Delta D_{jk}$$

where the force constants are defined in ref 54. A simple solution to the vibrational problem may be achieved by restricting $f_{DD}$ and $f_{dD}$ to zero. The resulting values of the force constants and the potential energy distributions are given in Tables XIV and XV, respectively (supplementary material). Of course, the central force constants may be easily obtained from the valence force constants with incorporation of the approximations in the respective potential fields given above with use of the following expressions, which relate the different types of force constants:

$$f_r + 2f_{rr} + f_{rr}' = f_d + f_D + 2f_{dd} + f_{dd}' + f_{DD} + 4(2^{1/2})f_{dD}$$

$$f_r - 2f_{rr} + f_{rr}' = f_d - 2f_{dd} + f_{dd}'$$

$$4f_\alpha - 8f_{\alpha\alpha} + 4f_{\alpha\alpha}' = f_D - f_{DD}$$

$$f_r - f_{rr} - 4f_{r\alpha} + 4f_{r\alpha}' + 2f_\alpha - 2f_{\alpha\alpha}' = f_d - f_{dd}'$$

**Registry No.** $Se_4^{2+}$, 12310-32-6; $Se_4(Sb_2F_4)(Sb_2F_5)(SbF_6)_5$, 82434-40-0; $Se_4(AsF_6)_2$, 53513-64-7; $Se_4(AlCl_4)_2$, 12522-25-7; $Se_4(HS_2O_7)_2$, 35025-26-4; $S_4(S_2O_6F)_2$, 82582-32-9; $KS_2O_6F$, 14325-72-5; $HS_2O_6F$, 23754-83-8; $S_4(SO_3F)_2$, 82582-30-7; $Te_4^{2+}$, 12597-50-1; $Te_4(AsF_6)_2$, 12536-35-5; $Te_4(SbF_6)_2$, 82292-92-0; $Te_4(AlCl_4)_2$, 12522-27-9; $Te_4(Al_2Cl_7)_2$, 36645-21-3; *trans*-$Te_2Se_2^{2+}$, 68652-59-5; *trans*-$Te_2Se_2^{2+}(Sb_3F_{17}^-)(SbF_6^-)$, 68791-83-3.

**Supplementary Material Available:** Listings of the central force constants (Table XIV) and potential energy distributions (Table XV) for the $S_4^{2+}$, $Se_4^{2+}$, and $Te_4^{2+}$ polyatomic cations (2 pages). Ordering information is given on any current masthead page.

(52) Teranishi, R.; Decius, J. C. *J. Chem. Phys.* **1954**, *22*, 896.
(53) Cyvin, S. *Acta Polytechn. Scand., Phys. Incl. Nucleon. Ser.* **1960**, *6*, 1.
(54) In the central forces potential field the force constants are defined as follows: $f_d$, chalcogen–chalcogen stretch (directly bonded); $f_{dd}$, stretch–stretch interaction (adjacent); $f_{dd}'$, stretch–stretch interaction (opposite); $f_D$, chalcogen–chalcogen stretch (diagonal); $f_{DD}$, stretch (diagonal)–stretch (diagonal) interaction; $f_{dD}$, stretch (directly bonded)–stretch (diagonal) interaction.

---

Contribution from the Shanghai Research Institute of Petrochemistry, Shanghai 201207, People's Republic of China

# Electronegativities of Elements in Valence States and Their Applications. 1. Electronegativities of Elements in Valence States

YONGHE ZHANG

*Received January 8, 1982*

The electronegativities of the elements in valence states are calculated on the basis of electrostatic force by using observed ionization potentials and covalent radii as main parameters. The ligand field stabilization, the first filling of p orbitals, the transition-metal contraction, and the lanthanide contraction are reflected in the relative values of the electronegativity scale. It is concluded that the electronegativities for the elements situated after the transition series produce the series second period $\gg$ third period $\approx$ fourth period $>$ fifth period $\approx$ sixth period.

## Introduction

Electronegativity is a important concept in understanding the chemical bond. It has unique and valuable applications to the interpretation of a vast area of common chemistry.

Pauling first defined electronegativity and suggested methods for its estimation in 1932.[1] Over the years, various other methods have been proposed for evaluating the electronegativity values of the elements. Only one method, proposed by Allred and Rochow,[2] has been widely accepted as an alternative to Pauling's thermochemical scale. Nevertheless, the concept of electronegativity is not precisely perfect and remains largely qualitative. As we shall see, the electronegativity values so determined can only be average ones for an atom's most common valence state and oxidation state cannot be appropriate when applied for quantitative applications. Besides, as the effective nuclear charges adopted in the Allred–Rochow method are from the simplified Slater rule,[3] in which the variations in atomic orbitals with increasing nuclear charges are ignored, this method cannot yet conform itself to some chemical facts; for instance, its electronegativities of the post-scandide elements (from Ga to Kr) are too high and those of the post-lanthanide elements from Tl to Rn) are too low. Although the concept is qualitatively valuable, the attempts to derive a comprehensive quantitative scale of electronegativity have been disappointing because of the lack of correlation between experimental quantities and the scale over a wide front.

(1) L. Pauling, *J. Am. Chem. Soc.*, **54**, 3570 (1932).
(2) A. L. Allred and E. G. Rochow, *J. Inorg. Nucl. Chem.*, **5**, 246 (1958).
(3) J. C. Slater, *Phys. Rev.*, **36**, 57 (1930).

0020-1669/82/1321-3886$01.25/0 